



IRI Data Used in Optimum Pavement Rehabilitation Models for Developing Countries: Palestine as a Case Study

Khaled A. Abaza¹ · Nizar A. Assi¹

Received: 10 August 2023 / Revised: 15 November 2023 / Accepted: 1 December 2023
© The Author(s), under exclusive licence to the Iran University of Science and Technology 2024

Abstract

This paper investigates the potential use of the International Roughness Index (IRI) in generating optimal rehabilitation plans at the network-level. The IRI data used in the study was obtained using the portable vehicle-mounted IRIMETER-2 profilometer, which is a product of Englo LLC, Tallinn, Estonia. An optimum rehabilitation model is proposed to minimize the average IRI value at the network-level subject to variable and budget constraints. The model mainly focuses on using major rehabilitation strategies that can produce a major improvement in pavement condition. An alternate maximization model that can use other pavement condition indicators, such as the present serviceability index (PSI) and pavement condition index (PCI), is also presented. The PSI and PCI can be estimated from the IRI using correlation models. The proposed optimum models are linear in form and can easily be solved using the proposed cost-effectiveness ratio. The sample results presented for a 27.1-km suburban highway indicate the reliability of using the IRI data to generate optimal rehabilitation plans. A statistical uncertainty analysis of IRI measurements produced a mild impact on optimal solutions derived using ten independent IRI tests and 99% confidence level. The uncertainty analysis has also indicated that the use of a single IRI test provides results that are statistically indifferent from those obtained using ten IRI tests.

Keywords Roadway roughness · Pavement rehabilitation · Pavement management · Optimization · Uncertainty analysis

1 Introduction

The main purpose of pavement management is to yield an optimal maintenance and rehabilitation (M&R) plan at the network-level. It generally requires optimizing the pavement condition while taking into account available resources, especially financial ones. Therefore, the pavement management problem is mainly an optimization problem that needs to be formulated using a specified decision-making policy subject to certain constraints. The optimization problem can be solved for a single time-horizon typically taken as one year, or an analysis period comprised of multiple time horizons, such as five years or more. A single time-horizon only requires present

pavement performance data, whereas multiple time-horizons require future pavement performance data for the specified analysis period. The latter case requires using a prediction model to generate future pavement performance data so that the optimization problem can be solved for each time horizon within the analysis period, thus resulting in what is known as a long-term M&R schedule [1, 2]. Several types of deterministic and probabilistic prediction models have been used in pavement management such as regression-based, Bayesian, Markov chain, and Artificial Neural Network (ANN) models [3–8].

Therefore, it is clear that reliable pavement performance data is the key requirement for yielding an effective M&R plan regardless of any proposed decision-making policy. Pavement performance or serviceability has typically been measured using either visual inspection or expensive instruments operated by well-trained staff such as the profilograph for pavement longitudinal roughness and falling weight deflectometer (FWD) for surface deflection measurements [9, 10]. While visual inspection is much less costly, it can involve significant variations in performance

✉ Khaled A. Abaza
kabaza@birzeit.edu

Nizar A. Assi
naassi@birzeit.edu

¹ Civil Engineering Department, Birzeit University,
West Bank, Palestine

measurements due to subjectivity. Also, visual inspection is time-consuming and associated with safety risks. Recent approaches to measuring pavement performance have focused on using automatic rather than manual data collection because it requires substantially less time and cost, and it is hazard-free and subjectivity-free [11, 12]. The outcome of pavement performance assessment is typically converted into a single pavement performance indicator, such as the present serviceability index (PSI), the pavement condition index (PCI), or the international roughness index (IRI). These sample performance indices have been extensively used in several pavement management applications [13–16].

A typical M&R plan can involve routine maintenance, such as crack sealing, pothole patching, and surface treatments such as sand and slurry seals. However, these routine maintenance treatments cannot significantly extend the pavement service life, nor can they cause major improvement in the present pavement condition [17, 18]. However, major rehabilitation actions, such as plain overlay, cold milling and overlay, and reconstruction can produce a major uplift in the pavement structural capacity, thus substantially extending the pavement service life. Consequently, most pavement management models have attempted to optimize pavement conditions at the network-level by mainly incorporating major rehabilitation strategies similar to the ones mentioned earlier [19–22].

The use of the IRI in the proposed rehabilitation model at the network-level can be particularly beneficial for planning purposes. However, once projects are selected for implementation, then a structural-based assessment can be performed at the project-level to specify the appropriate rehabilitation strategy (i.e., overlay/reconstruction/etc.). Structural-based assessment may involve deflection tests, Marshall tests, bearing capacity tests, etc. depending on local affordability. Nevertheless, highway agencies with limited resources may not be able to afford expensive material testing, and they typically rely on “prescription” procedures developed based on experience and engineering judgment. Alternatively, the PCI can be used in lieu of the IRI since it mostly accounts for the pavement’s structural integrity. The PCI can be field-estimated based on the assessment of pavement distress or obtained from the IRI measurements using correlation models as later presented.

The use of IRI data in developing an optimal rehabilitation plan is suitable for developing countries because the instruments and methods used for collecting IRI data are cost-effective. Generally, developing countries, especially those with limited financial resources, cannot afford to purchase and operate sophisticated instruments for IRI measurements. The purchase cost of the instrument used in this study is affordable (about 15,000 USD). The device is a portable one that can be easily installed and operated

using an automobile. The device can be operated at a wide range of speeds (20–100 km/hr), making it appropriate to cover a road network with different speed limits. Therefore, the operation time and cost associated with IRI collection for a road network is reasonably low. Also, the proposed optimum pavement rehabilitation model using IRI data does not require advanced technical expertise to formulate and solve.

The key research objective of this paper is to investigate the potential use of IRI data in generating an optimum rehabilitation plan at the network-level. The IRI was proposed by the World Bank as an international standard statistic to quantify pavement performance used in pavement management applications [23]. It is a measure of the longitudinal profile roughness defined in relation to the cumulative suspension motion associated with a moving vehicle over a traveled distance [9]. Therefore, it essentially describes the vehicle vibrations caused by the profile roughness expressed in the unit of (m/km). Traditional methods for measuring the IRI rely on expensive instrumentation and require well-trained professionals, thus limiting the use of these instruments at the network-level. Furthermore, the associated testing procedure is time-consuming and labor-intensive. In contrast, modern portable instruments for measuring the IRI mainly rely on using sensors to quantify vehicle vibrations so that higher vehicle vibrations will result in higher IRI values [23].

Generally, two approaches, direct and indirect, have been reported in the literature for measuring the longitudinal profile roughness in order to represent the IRI [24, 25]. The direct approach requires conducting roadway longitudinal surveys using rod and level or advanced laser-type profilometers. The indirect approach mainly deploys response-type roughness meters that calculate the total simulated vehicle suspension motion to be divided by the traveled distance to yield the average suspension motion per unit length. The vehicle-simulated suspension is typically computed using a mathematical quarter-car vehicle model [23]. The indirect approach is commonly used worldwide because of its effectiveness in terms of saving time and money and is considered hazard-free. Several portable IRI measuring devices have been developed utilizing the indirect approach. The IRIMETER-2 used in this study is one example.

There are five main objectives associated with this research paper as follows:

1. Applying IRIMETER-2 profilometer to obtain IRI measurements at the network-level.
2. Searching the literature for sample correlation models that can be used to estimate the PSI and PCI from IRI.
3. Proposing an optimum rehabilitation model that seeks to optimize the pavement condition at the network-

- level with IRI measurements being the main data requirement.
4. Proposing a similar optimum rehabilitation model that can make use of other pavement condition indicators such as the PSI and PCI. The focus is mainly on optimal solutions for a single time-horizon.
 5. Investigating the uncertainty impact of IRI measurements on the optimal solutions obtained using the three outlined pavement condition indicators (i.e., IRI/PSI/PCI). Also, investigating the uncertainty impact of the sample size as related to the number of required IRI tests.

Figure 1 provides a flowchart that presents the main objectives associated with this research along with their logical sequence.

2 Literature Review of IRI Research

The IRI is a universal standard for pavement roughness measurement and it has become the most widely used road condition indicator. Múčka [26] summarizes the IRI limit values for different pavement types including new and rehabilitated/reconstructed pavements. Limit values are found to be a function of road surface type, road functional category, road speed limit, road construction type, or average annual daily traffic (AADT). Several IRI-related studies can be found in the literature with an emphasis on improving the methods used to estimate the IRI. For

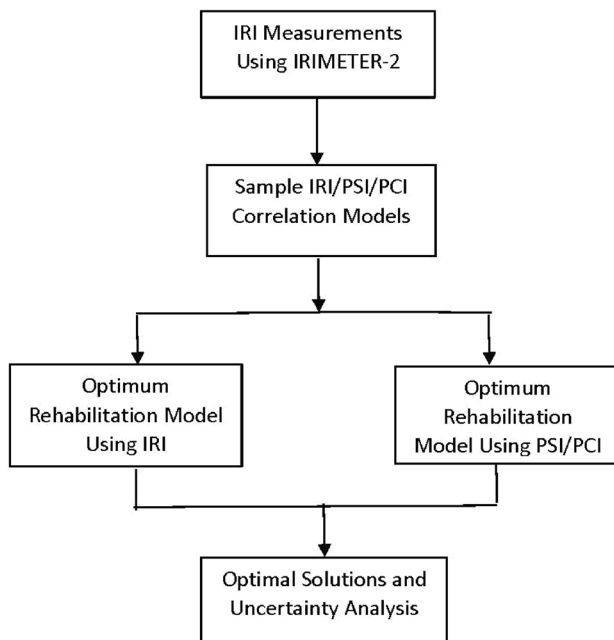


Fig. 1 Definition and logical sequence of the five main research objectives

example, Sidess et al. [27] proposed a model to predict the deterioration of the IRI over time. The model is a function of pavement structural parameters such as structural number, asphalt layer thickness, subgrade strength, and environmental conditions. The approach used in model development is based on a combination of empirical-mechanistic and regressive-empirical.

Moreover, Šroubek et al. [28] proposed and derived a new numerical method for IRI computation. The method does not use iterative approximation as originally proposed by Sayer's method [23]. This makes the new method much faster especially for road data that is not uniformly sampled. Mirtabar et al. [29] proposed a new vibration-based approach to estimate the IRI. The new method uses a low-cost three-axis Micro-Electro-Mechanical Systems accelerometer and a Global Positioning System sensor. The pavement profile is obtained by double integration of z-axis acceleration data with the IRI being computed using process valves and automation system software. Abdelaziz et al. [30] proposed an IRI prediction model for flexible pavement using multiple-linear regression and artificial neural networks (ANNs). The model predicts the IRI as a function of pavement age, initial IRI value, transverse cracks, alligator cracks, and rut depth standard deviation. Pérez-Acebo et al. [31] used the Markov chain to predict the future IRI values for flexible pavement based on IRI measurements collected twice a year. Consequently, relevant transition probability matrices were developed using a half-year cycle length.

The main objective of this paper is to use IRI data in a simple pavement management model capable of yielding optimal solutions at the network-level. The proposed model is linear in form and can be easily solved by pavement engineers. The other similar studies generally proposed sophisticated models that are more data-demanding and require solutions using advanced optimization methods. A sample of these advanced methods, which mainly focuses on using the IRI in relevant pavement management applications, is summarized below.

Khattak et al. [32] used IRI data to develop predictive models for HMA overlay treatment of flexible and composite pavements. The predictive models are useful in support of cost-effective selection of pavement treatment type and timing. Loprencipe et al. [33] applied IRI data to develop a sustainable pavement management system that accounts for vehicle operating costs. The system provides highway managers with a tool to compare alternative maintenance strategies and perform priority analysis at the network-level. Saha and Ksaibati [34] developed a risk-based optimization methodology for pavement management of county paved roads. The proposed methodology can identify the best mix of keeping projects within budget, maximizing traffic on treated roads, maximizing the

weighted PSI/IRI average, and minimizing risk. Janani et al. [35] proposed a novel method to prioritize pavement sections for maintenance and rehabilitation actions using only functional performance indicators, such as the IRI. The proposed method allows pavement engineers to considerably reduce the frequency of expensive, time-consuming, and traffic-disruptive tests for obtaining the structural characteristics of pavements. In addition, several international highway agencies have used the IRI as a key pavement performance indicator in their pavement management systems [36–38].

3 IRIMETER-2 Setup and Specifications

The IRIMETER-2 is a vehicle-mounted device for road roughness measurements. It is a product of Englo LLC, Tallinn, Estonia. The device is designed to compute the IRI for a 5-m roadway lane length. The main device components are a control unit with a graphic LCD display, two wireless inertial sensors, and a roof magnet-mounted GPS antenna. The two wireless sensors are to be installed on the vehicle's front axle, one next to each wheel. Each sensor can detect and record the vehicle suspension motion, which is then converted into an IRI value. The two IRI values from the two sensors are averaged out to give a single IRI value for each 5-m lane length. The sensors are wirelessly connected to the rest of the system. Figure 2 shows pictures of the device's three main components. The GPS unit is an important feature as it allows assigning the IRI measurements to their specific locations with outcomes displayed on actual maps of the road network.

The IRIMETER-2 system can be easily mounted on any passenger car; preferably, if its suspension system is at least in fair condition. It can be operated on both paved and unpaved roads under all weather conditions provided the vehicle speed is in the range of 20–100 km/hr. This wide speed range allows the operator to select the speed that is consistent with the road speed limit; however, it is recommended to maintain approximately the same speed for a given roadway. The IRIMETER-2 operating system is designed to store IRI measurements for up to 15,000 lane-kilometer. The stored data can be downloaded to a computer via a USB connection. The system software allows the user to manipulate and analyze the IRI data with results displayed using graphs, tables, and maps. Figure 3 shows sample IRI display formats. The IRIMETER-2 system is very portable with only a 2 kg total weight. It provides IRI measurements with 0.1 resolution.

The IRIMETER-2 has a reasonable purchase price of about 15,000 USD, which makes it affordable especially for developing countries with limited financial resources. The operating cost is also minimal as it only requires a

passenger car with a driver and a professional staff, preferably an engineer or technician who can operate the IRIMETER-2 software to retrieve and analyze the IRI data. Birzeit University, Birzeit, Palestine, has recently acquired an IRIMETER-2 device to be mainly used in research activities. One main research objective is to investigate the feasibility of using IRI measurements in developing reliable optimal rehabilitation plans at the network-level. Therefore, sample IRI data for a 27.1 km major suburban highway is presented and used to yield optimal solutions via an optimization model. The proposed optimization model is capable of either minimizing the network average IRI value or maximizing the network average PSI/PCI value as outlined next.

4 Methodology

The methodology section has two parts. The first presents the optimum rehabilitation models proposed to yield optimal solutions at the network-level using major rehabilitation actions with pavement performance defined using either IRI, PSI, or PCI. The proposed models are designed to generate optimal solutions for a single time horizon as would typically be the case in developing countries such as Palestine. The second section presents sample correlation models amongst the three outlined condition indicators, namely IRI, PSI, and PCI. This allows a developing country interested in using PSI/PCI to still use the proposed relevant optimum model.

4.1 Optimum Rehabilitation Model

The optimum decision-making policy for the development of an optimal rehabilitation plan is generally based on optimizing the network pavement condition. This can be achieved by minimizing the average IRI value associated with a particular pavement network. The IRIMETER-2 device used in this study estimates the IRI value for consecutive pavement sections with a 5-m lane length. The software associated with the device can provide a summary of the IRI results using different IRI ranges as specified by the user. As part of the result summary, the number of 5-m pavement sections within each IRI range (i.e., class) can be obtained (N_{ij}) for the i th class and j th test. The average number of pavement sections in the i th class (\bar{N}_i) is computed from the section numbers (N_{ij}) obtained using (n) tests as indicated by Eq. (1). Each pavement section represents one IRI measurement point corresponding to a 5-m lane length.

$$\bar{N}_i = \frac{\sum_{j=1}^n N_{ij}}{n} \quad (1)$$



(A) Control unit with graphic LCD display mounted on vehicle dashboard.



(B) Wireless inertial sensor mounted to each wheel-support assembly.



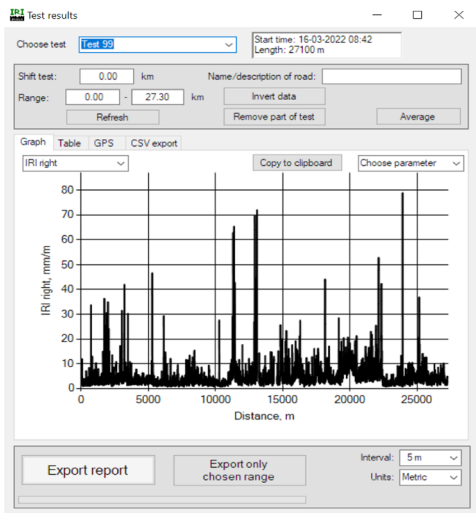
(C) Magnet GPS antenna mounted on vehicle's roof.

Fig. 2 Main IRIMETER-2 components

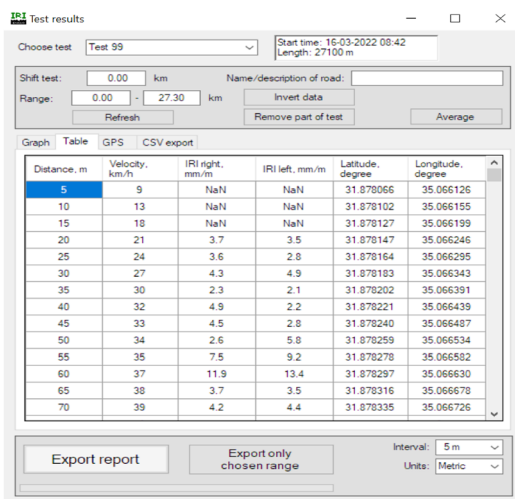
Similarly, the average IRI value of the i th class (\overline{IRI}_i) is calculated as the arithmetic average of the corresponding IRI averages ($\overline{IRI}_{i,j}$) associated with the j th test for a specific highway network as defined in Eq. (2).

$$\overline{IRI}_i = \frac{\sum_{j=1}^n \overline{IRI}_{i,j}}{n} \quad (2)$$

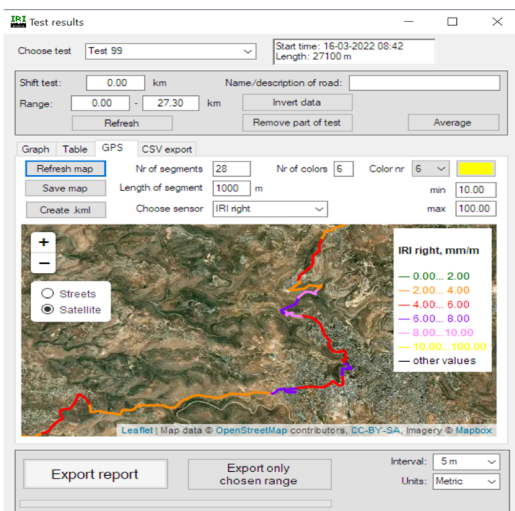
The average IRI value associated with a particular pavement network (\overline{IRI}_{net}) can be determined using Eq. (3). It is computed as a weighted average based on the average section numbers (\overline{N}_i) and average IRI values (\overline{IRI}_i) associated with (m) IRI classes, and a total number of pavement sections associated with a particular pavement network (N_T).



(A) Using graphical representation (distance versus IRI)



(B) Using tabular format



(C) Using map with GPS coordinates.

$$\overline{IRI}_{net} = \frac{1}{N_T} \sum_{i=1}^m \overline{N}_i \times \overline{IRI}_i, \text{ where } : N_T = \sum_{i=1}^m \overline{N}_i \quad (3)$$

The proposed optimum rehabilitation model requires that a potential major rehabilitation strategy be specified for pavement sections in each pavement class. It also requires defining the improvement expected to be gained by each pavement class (ΔIRI_i) in terms of the IRI value. This gain is defined as the difference between the class average IRI value (\overline{IRI}_i) and the class average IRI value expected after major rehabilitation (\overline{IRI}_o), which is assumed to be the same for all classes. The class IRI gains are to be multiplied by the corresponding class numbers of pavement sections to be rehabilitated (N_i) to yield the network average IRI value after major rehabilitation as presented in Eq. (4). The net gain in pavement condition improvement as a result of major rehabilitation is presented as a deduct term in Eq. (4). Therefore, Eq. (4) will yield a lower network average IRI value for a specific major rehabilitation strategy. According to Eq. (4), it is assumed that all pavement classes can receive major rehabilitation with the exception of class number 1 (i.e., the class with the best pavement condition). Typically, lower IRI values indicate better pavement conditions.

$$\overline{IRI}_{net} = \frac{1}{N_T} \left[\sum_{i=1}^m \overline{N}_i \times \overline{IRI}_i - \sum_{i=2}^m N_i \times \Delta IRI_i \right] \quad (4)$$

It is also popular to use other pavement condition indicators, such as the present serviceability index (PSI) and pavement condition index (PCI). However, the values of these condition indices increase with the application of pavement major rehabilitation. Therefore, the net gain in pavement condition improvement as a result of major rehabilitation is a positive one as indicated by Eq. (5). Equation (5) is similar to Eq. (4) but uses PSI as the pavement condition indicator. Equation (5) will yield a larger network average PSI value (\overline{PSI}_{net}) compared to the original case without any major rehabilitation.

$$\overline{PSI}_{net} = \frac{1}{N_T} \left[\sum_{i=1}^m \overline{N}_i \times \overline{PSI}_i + \sum_{i=2}^m N_i \times \Delta PSI_i \right] \quad (5)$$

In the search for an optimal rehabilitation plan, the numbers of pavement sections to be rehabilitated (N_i) in the various applicable pavement classes are considered as the variables to be optimized subject to budget and variable lower and upper-limit constraints. Equation (6) represents the objective function to be minimized when using the IRI as the pavement condition indicator.

$$\text{Minimize : } \overline{IRI}_{net} = \frac{1}{N_T} \left[\sum_{i=1}^m \overline{N}_i \times \overline{IRI}_i - \sum_{i=2}^m N_i \times \Delta IRI_i \right], \quad (6)$$

Fig. 3 IRI data display formats

where : $\Delta IRI_i = \overline{IRI}_i - IRI_o$

However, in the case of using the PSI as the pavement condition indicator, the goal is to maximize the pavement network average PSI value as defined in Eq. (7). Both Eqs. (6) and (7) represent linear models with (m-1) variables, namely the (N_i) variables. The solution for a linear optimization problem can be readily obtained using commercially available software packages.

Maximize : \overline{PSI}_{net}

$$= \frac{1}{N_T} \left[\sum_{i=1}^m \overline{N}_i \times \overline{PSI}_i + \sum_{i=2}^m N_i \times \Delta PSI_i \right], \quad (7)$$

where: $\Delta PSI_i = \overline{PSI}_i - PSI_o$

Both linear models presented in Eqs. (6) and (7) are subject to the following constraints:

- 1) $RC = 5W \sum_{i=2}^m (UC_i \times N_i) \leq AB$
- 2) $N_i \geq 0$
- 3) $N_i \leq \overline{N}_i$

The first constraint is the budget constraint, which requires that the major rehabilitation cost (RC) associated with a particular rehabilitation plan must be less than or equal to the allocated budget (AB). The RC is computed from the product sum of multiplying the rehabilitation cost units (UC_i in USD/m^2) by the corresponding number of pavement sections to be rehabilitated (N_i). This product sum is then multiplied by the travel lane width (W) in meters and pavement section length (i.e., 5 m). The second constraint is the variable non-negativity one. The third one enforces the variable upper-limit value as defined by the class average number of pavement sections (\overline{N}_i).

4.2 Sample IRI/PSI/PCI Correlation Models

The IRI as a pavement condition indicator mainly considers pavement surface roughness in the longitudinal direction, thus representing a measure of the pavement functional performance that greatly affects passenger discomfort. On the other hand, the PSI accounts partially for pavement structural performance as it considers both cracking and patching, although its value is largely controlled by pavement surface roughness [24]. On the contrary, the PCI value is largely controlled by structural defects, such as different types of cracking both load and non-load-related. Therefore, the PCI is mainly a measure of the pavement structural capacity, which is a key indicator of pavement load-carrying capability. Generally, all three previously outlined pavement condition indicators have been used in pavement rehabilitation and management applications [13–16]. However, the main advantage of

using the IRI is that the associated testing procedure is cost and time-effective, efficient, and safe.

Some researchers have developed correlation models to estimate one pavement condition indicator from the other ones. For example, Paterson [14] developed the predictive exponential model presented in Eq. (8), which can be used to estimate the PSI from the IRI (m/km) for flexible pavement structures. Another similar model was developed by Al-Omari and Darter [39] as presented in Eq. (9).

$$PSI = 5e^{-0.18IRI} \quad (8)$$

$$PSI = 5e^{-0.24IRI} \quad (9)$$

The PCI can be typically estimated for a particular pavement section using the procedure outlined by ASTM [40]. The relevant procedure requires assessing the extent and severity of a large number of pavement defects, with the result being a total deduct value that has to be subtracted from the perfect score of 100. The test procedure is time-consuming and is considered somewhat subjective. Similar to PSI, Park et al. [9] developed a power regression model as defined in Eq. (10) to estimate the PCI value from the corresponding IRI (m/km) for a particular pavement section. However, according to Eq. (10), the maximum value for PCI is only about 87.1, which might be somewhat restrictive. Also, Dewan and Smith [41] proposed a linear model to estimate the IRI from the PCI as presented in Eq. (11). However, this linear model resulted in a 0.53 R-square value.

$$PCI = 87.098IRI^{-0.481} \quad (10)$$

$$IRI = 0.0171 (153 - PCI) \quad (11)$$

Another model to estimate the PCI from the IRI was proposed by Park et al. [9], which also takes on a power form but is transformed into a linear logarithmic model as defined in Eq. (12). A boundary condition was set in developing this model by requiring a minimum IRI value of 0.727 to yield a maximum PCI value of 100. This required the zero intercept to be set at 2. Therefore, this model can yield PCI values up to 100; however, the model needs calibration using observed PCI and IRI values to estimate the K_2 coefficient, which should have a negative value so that the PCI value remains less than 100. The PCI can replace the PSI in Eq. (7) if so preferred.

$$\log PCI = 2 + K_2 \log \left(\frac{IRI}{0.727} \right), \text{ where : } IRI \geq 0.727 \quad (12)$$

Furthermore, Fuentes et al. [10] proposed a linear model to estimate the PSI as a function of both IRI and PCI as defined in Eq. (13). This model provides a logical inverse relationship between PSI and IRI and a direct relationship between PSI and PCI as one would expect. The earlier PSI

predictive models developed from the AASHTO road test gave much higher weight to roadway roughness compared to cracking and patching; however, these pavement defects inversely influenced the PSI estimation [42].

$$PSI = 4.22 - 0.24IRI + 0.013PCI \quad (13)$$

Recently, several other researchers have investigated the relationship between PCI and IRI. For example, Elhadidy et al. [43] used distress data from the LTPP database to develop a simplified model to estimate the PCI from the IRI. A sigmoid function was found to be effective in predicting PCI from IRI at a very high coefficient of determination ($R^2 = 0.995$). In another study, Adeli et al. [44] presented three linear models to estimate the PCI from the IRI using different IRI ranges with R^2 ranging from 0.59 to 0.76. Other researchers attempted to develop correlation models between the IRI as a functional indicator and structural indicators, namely deflection-based parameters (DBPs) [45]. Relevant sample data extracted from the LTPP was used to develop correlation models for two pavement structures (A and B) with 0.71 and 0.65 R-square values, respectively.

In general, it is recommended that correlation models similar to the previously outlined ones be developed based on local traffic conditions and material characteristics. Once these models are developed, a highway agency can have the choice of using any one of the three outlined pavement condition indicators (i.e., IRI, PSI, PCI) in developing an optimal rehabilitation plan as proposed in this paper.

The main objective of this research paper is to use IRI data in developing optimal rehabilitation strategies at the network-level [46]. Moreover, other pavement condition indicators, such as the PSI and PCI, can be used if so preferred. While both PSI and PCI can be field estimated using published procedures [40, 42], they can also be obtained from IRI measurements using already published correlation models. The PSI as defined in the original AASHTO model is a function of pavement roughness, cracking, and patching [42]. However, cracking and patching only contributed about 5% to the model correlation coefficient [24]. Therefore, potential predictive models have only used the IRI to estimate the PSI [14, 39].

5 Sample Presentation

The sample presentation section includes three subsections, namely IRI measurements obtained using IRIMETER-2, developing sample optimal rehabilitation plans using optimum models presented in Eqs. (6) and (7), and uncertainty analysis to investigate the impact of variation

in the IRI measurements on optimal solutions obtained using ten independent IRI tests.

5.1 IRI Measurements via IRIMETER-2

The IRIMETER-2 device was used to evaluate the present pavement roughness of a two-lane suburban highway located in the district of Ramallah, Palestine. Figure 4 provides a location map for the highway under investigation. The highway has a total length of 27.1 km. It has a flexible pavement structure with a 12-cm asphalt concrete surface. The pavement longitudinal roughness was tested ten times (n) in each highway direction using the IRIMETER-2 device. Each test was run by driving the vehicle within the two visible wheel tracks so that the impact of vehicle lateral wandering on roughness measurements could be minimized. The IRIMETER-2 device measures the IRI value for pavement sections with a 5-m lane length. The IRI results obtained for the ten tests are summarized using six different pavement classes as provided in Tables 1 and 2 for both the forward and backward highway directions, respectively. The tables provide the numbers of 5-m pavement sections (i.e., measurement points), $N_{i,j}$, associated with the 6 pavement classes considering each IRI test.

It can be noticed that there are some variations in the number of measurement points ($N_{i,j}$) associated with the ten tests when considering the same pavement class, which can be mainly attributed to vehicle lateral wandering. The average number of measurement points (\bar{N}_i) associated with each pavement class is provided at the bottom of Tables 1 and 2. There are some variations in the average number of measurement points (\bar{N}_i) as relevant to both highway directions, which can be expected. However, the overall assessment is that both highway directions are in a state of similar longitudinal roughness as indicated by the class percentages provided at the bottom of the tables.

Table 3 provides a summary of statistics associated with both highway directions combined. It includes the total number of measurement points (\bar{N}_i) to be used in developing the optimal rehabilitation plan as outlined earlier. It also provides the class average IRI value (\overline{IRI}_i) computed as the arithmetic average of all IRI values associated with the total number of measurement points (\bar{N}_i). The standard deviation (S_i) associated with all IRI values is also provided for each pavement class. The three outlined statistics (i.e., \bar{N}_i , \overline{IRI}_i , S_i) have been used in Eqs. (14) and (15) to establish the class upper and lower-limit average IRI values (\overline{IRI}_{u_i} & \overline{IRI}_{l_i}), respectively, to investigate the uncertainty impact of IRI measurements on the derived optimal rehabilitation plans. The standard normal variable ($Z_{\alpha/2}$) is used in Eqs. (14) and (15) since the sample size (\bar{N}_i) is

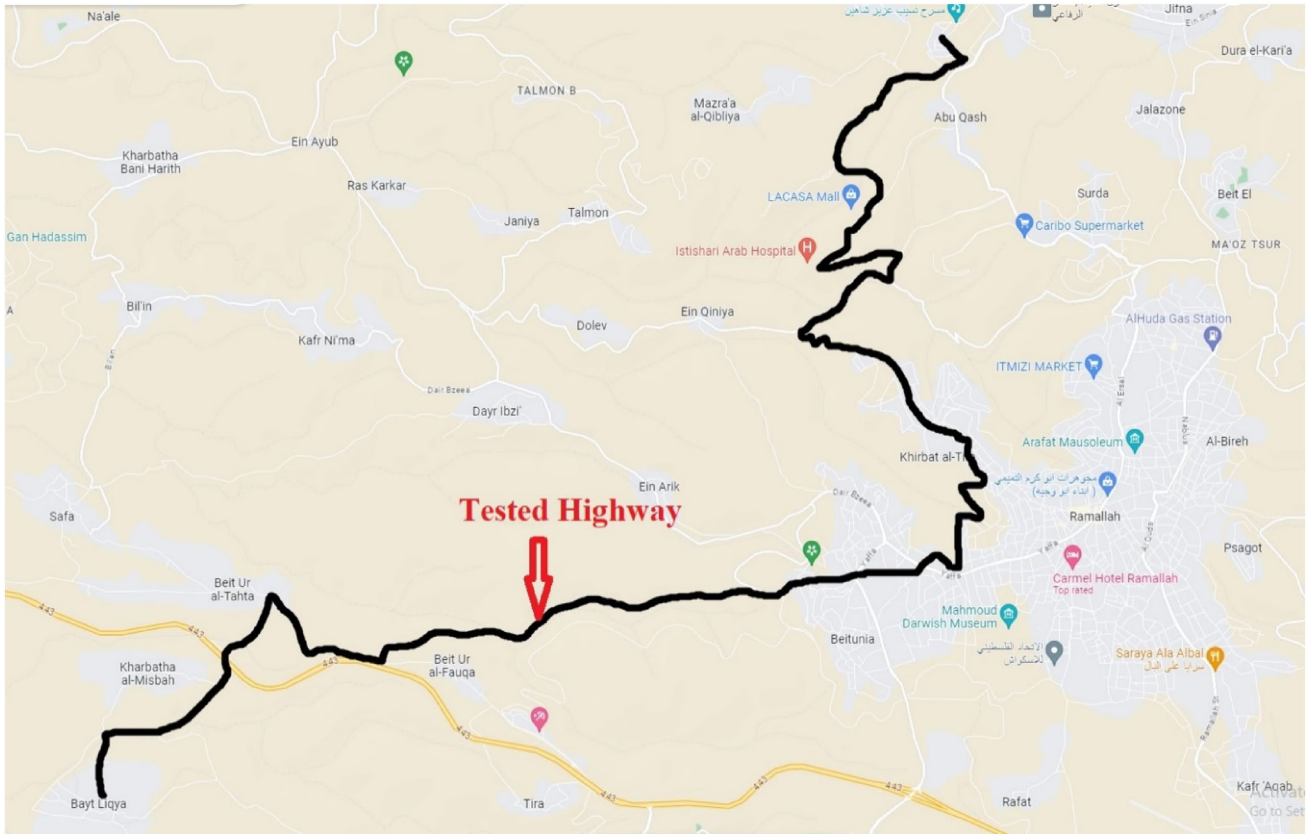


Fig. 4 Location map of tested highway, Ramallah district, Palestine

Table 1 IRI measurement points for highway forward direction

Test No. (j)	IRI measurement points (N_{ij}) for i^{th} class						Total
	IRI = 0–2 Class 1	2–4 Class 2	4–6 Class 3	6–8 Class 4	8–10 Class 5	IRI > 10 Class 6	
1	891	2385	1018	515	266	345	5420
2	851	2372	1064	505	283	345	5420
3	814	2415	1025	528	271	367	5420
4	832	2409	1054	513	250	362	5420
5	811	2434	1075	493	250	357	5420
6	863	2335	1103	503	284	332	5420
7	810	2390	1114	479	290	337	5420
8	772	2408	1115	528	252	345	5420
9	821	2357	1059	496	296	391	5420
10	850	2460	1059	470	253	328	5420
Mean (\bar{N}_i)	832	2396	1069	503	269	351	5420
Class %	15.35	44.21	19.72	9.28	4.96	6.48	100%

larger than (30) with its value being equal to (2.58) for a 99% confidence level. It can be noticed that the standard deviation for class 6 is substantially larger than the corresponding values associated with the other classes because class 6 covers a much wider range of IRI data. However, the corresponding 99% confidence IRI range [14.76, 16.22]

is somewhat narrow due to the relatively large sample size (\bar{N}_i).

$$\overline{IRI}u_i = \overline{IRI}_i + Z_{\alpha/2} \frac{S_i}{\sqrt{\bar{N}_i}} \tag{14}$$

Table 2 IRI measurement points for highway backward direction

Test No. (j)	IRI measurement points ($N_{i,j}$) for i^{th} class						Total
	IRI = 0–2 Class 1	2–4 Class 2	4–6 Class 3	6–8 Class 4	8–10 Class 5	IRI > 10 Class 6	
1	722	2600	1131	440	236	291	5420
2	720	2547	1154	442	249	308	5420
3	675	2600	1135	444	250	316	5420
4	608	2476	1209	508	262	357	5420
5	652	2550	1215	497	217	289	5420
6	718	2577	1114	471	244	296	5420
7	722	2555	1128	462	254	299	5420
8	748	2558	1107	432	241	334	5420
9	745	2559	1129	436	234	317	5420
10	626	2529	1193	494	256	322	5420
Mean (\bar{N}_i)	694	2555	1151	463	244	313	5420
Class %	12.82	47.14	21.23	8.54	4.50	5.77	100%

Table 3 IRI/PSI statistics for both highway directions combined

Statistic	Statistic value						Total
	IRI = 0–2 Class 1	2–4 Class 2	4–6 Class 3	6–8 Class 4	8–10 Class 5	IRI > 10 Class 6	
Mean (\bar{N}_i)	1526	4952	2220	966	514	664	10,840
\overline{IRI}_i (m/km)	1.63	2.94	4.88	6.90	8.90	15.49	–
S_i (m/km)	0.27	0.56	0.57	0.57	0.58	7.32	–
$\overline{IRI}u_i$	1.65	2.96	4.91	6.95	8.97	16.22	–
$\overline{IRI}l_i$	1.61	2.92	4.85	6.85	8.83	14.76	–
\overline{PSI}_i	3.73	2.95	2.08	1.44	1.01	0.31	–
$\overline{PSI}u_i$	3.72	2.93	2.07	1.43	0.99	0.27	–
$\overline{PSI}l_i$	3.74	2.96	2.09	1.46	1.00	0.35	–

$$\overline{IRI}l_i = \overline{IRI}_i - Z_{\alpha/2} \frac{S_i}{\sqrt{N_i}} \quad (15)$$

5.2 Sample Optimal Rehabilitation Plans

The implementation of the proposed optimum rehabilitation model requires defining the potential major rehabilitation strategies to be applied to various pavement classes. Table 4 provides the definitions of five major rehabilitation strategies to be applied to pavement classes (2–6) with class 1 being excluded from any major rehabilitation work as outlined earlier. These major rehabilitation strategies range from 2.5-cm thin hot-mix asphalt (HMA) overlay applied to class 2 to reconstruction, which typically includes completely removing the existing asphalt surface, providing a leveling aggregate course, and placing a 12-cm

HMA surface to pavements in class 6. Table 4 also provides the cost units (UC_i), in US dollars per square meter of pavement surface area, for the proposed major rehabilitation strategies estimated based on local prices for performing similar rehabilitation work. The amount of work to be done in each pavement class is represented by the corresponding rehabilitation variable (N_i), which defines the number of 5-m pavement sections to receive the relevant rehabilitation strategy.

The number (N_i) needs not be an integer because rehabilitation work can involve a section portion. Therefore, it is not required to solve the optimum models proposed in Eqs. (6) and (7) as integer linear programs. They can be simply solved as linear programs using commercially available software packages. The software package called “Maple 7” was used in this sample presentation to yield sample optimal solutions for the optimum linear models

Table 4 Definition of various pavement classes and applicable rehabilitation plans

Class i	IRI range (m/km)	Rehabilitation strategy	Rehab. variable	Cost unit (UC _i), USD/m ²
1	0–2	– ^a	–	–
2	2–4	2.5 cm HMA overlay	N ₂	8
3	4–6	3.5 cm HMA overlay	N ₃	12
4	6–8	5.0 cm HMA overlay	N ₄	17
5	8–10	6 cm cold milling + 6 cm HMA overlay	N ₅	28
6	> 10	removal of existing asphalt layer, adding aggregate leveling course, and placing 12 cm HMA surface	N ₆	46

^a Not applicable

presented in Eqs. (6) and (7). The objective function presented in Eq. (6) requires the deduction of the improvement gain (ΔIRI_i), which has been computed assuming the IRI value after rehabilitation is equal to one ($IRI_o = 1.0$) for all rehabilitation strategies. The initial IRI value (IRI_o) is to be practically determined by testing the newly rehabilitated pavement using the IRIMETER-2 device. In this sample presentation, it was estimated to be about one.

The application of Eq. (7) requires estimating the PSI values for various deployed pavement classes. Table 3 provides the mean, lower, and upper-limit PSI values computed from Eq. (8) using the corresponding mean, lower, and upper-limit IRI values. The added class improvement gains (ΔPSI_i), as required by Eq. (7), are

computed using an initial ($PSI_o = 4.18$) value obtained from Eq. (8) based on an initial ($IRI_o = 1.0$) value. It is to be noted that higher PSI values correspond to lower IRI values as expected. Higher PSI/lower IRI value is an indication of superior pavement condition. A class cost-effectiveness (CE_i) parameter is presented in Eqs. (16) and (17), which is defined as the ratio of pavement improvement gain to rehabilitation cost unit (UC_i). Therefore, the higher the CE_i value, the more cost-effective is the corresponding rehabilitation strategy. It is later demonstrated that CE_i has a vital impact on the derivation of optimal solutions obtained using Eqs. (6) and (7).

$$CE_i = \frac{\Delta IRI_i}{UC_i} = \frac{\overline{IRI}_i - \overline{IRI}_o}{UC_i} \tag{16}$$

$$CE_i = \frac{\Delta PSI_i}{UC_i} = \frac{\overline{PSI}_i - \overline{PSI}_o}{UC_i} \tag{17}$$

Sample CE_i values are computed for the IRI/PSI data provided in Table 3 considering mean, lower, and upper-limit values. Figure 5 depicts the relevant CE_i values for the 6 pavement classes using the IRI as the condition indicator. The lowest CE_i is associated with class 2 whereas the highest value corresponds to class 4. Similarly, Fig. 6 shows sample CE_i values using the PSI with lowest and highest values corresponding to classes 6 and 3, respectively. It can be noted from Figs. 5 and 6 that there are minor differences in CE_i values considering mean, lower, and upper-limit values. The only exception is the case associated with class 6 shown in Fig. 5, which is attributed to the much larger standard deviation (S_i). Another observation is the CE_i values provided in Fig. 5 are larger than the corresponding ones given in Fig. 6. This

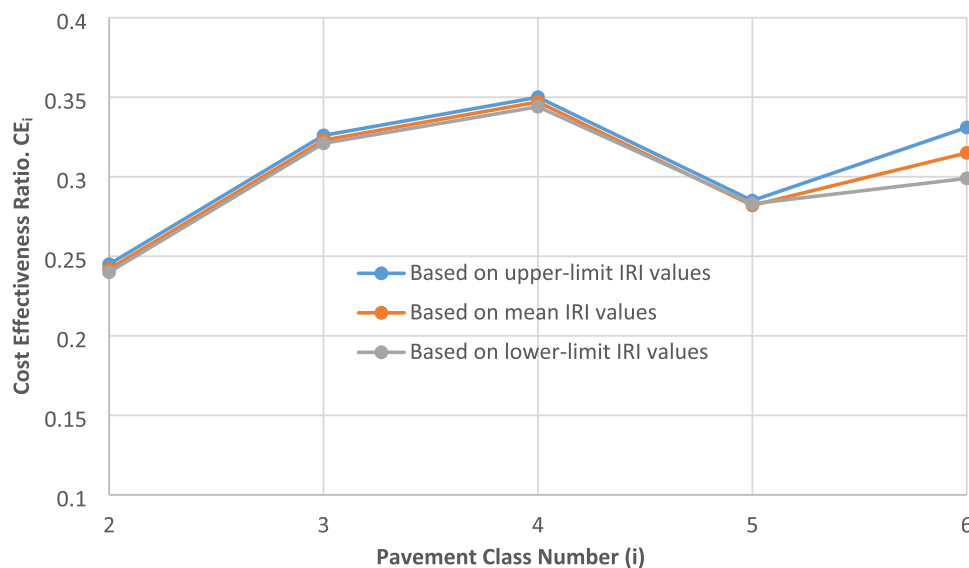


Fig. 5 Sample (CE_i) values obtained using IRI as the pavement condition indicator

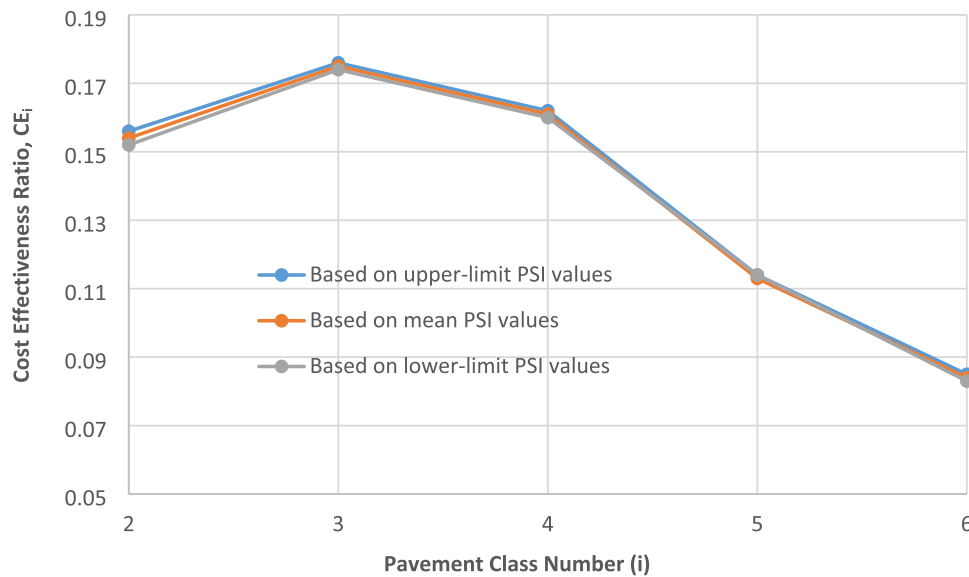


Fig. 6 Sample (CE_i) values obtained using PSI as the pavement condition indicator

Table 5 Sample optimal rehabilitation plans for minimizing (\overline{IRI}_{net}) using mean IRI values

Annual budget (USDx10 ⁶)	Optimal Solutions					
	$N_{2'}$	$N_{3'}$	$N_{4'}$	$N_{5'}$	$N_{6'}$	\overline{IRI}_{net} (m/km)
0.0	0	0	0	0	0	4.56
0.25	0	0	840.3	0	0	4.10
0.5	0	1012.4	966	0	0	3.67
1.0	0	2220	966	0	306.1	2.83
1.5	0	2220	966	432.4	664	2.03
2.0	3286	2220	966	514	664	1.39

Table 6 Sample optimal rehabilitation plans for maximizing (\overline{PSI}_{net}) using mean PSI values

Annual budget (USDx10 ⁶)	Optimal solutions					
	$N_{2'}$	$N_{3'}$	$N_{4'}$	$N_{5'}$	$N_{6'}$	\overline{PSI}_{net}
0.0	0	0	0	0	0	2.49
0.25	0	1190.5	0	0	0	2.72
0.5	0	2220	113.6	0	0	2.95
1.0	1760.1	2220	966	0	0	3.37
1.5	4952	2220	966	108.4	0	3.76
2.0	4952	2220	966	514	374.2	4.01

is because the practical IRI range is larger than the PSI range.

Table 5 provides sample optimal solutions ($N_{i'}$) obtained for different allocated budgets (AB) using the mean IRI value (\overline{IRI}_i). The optimal solutions have been obtained by solving the optimum linear model presented in

Eq. (6) using the software package called “Maple 7.” It can be noted that only the optimal variable ($N_{4'}$) with the highest (CE_i) value has been selected when assigning a budget of \$0.25 million. When the allocated budget increased to \$0.5 million, the optimal solution picked another optimal variable ($N_{3'}$), which is the one associated with the next highest (CE_i) value. However, this happened after the optimal variable ($N_{4'}$) with the highest (CE_i) value had been fully utilized (i.e., $N_{4'} = \overline{N}_4$). The same logic continued in identifying the optimal solutions with the increase in the allocated budget. This means the optimal solution will pick the variable with the highest (CE_i) value provided the ones with higher (CE_i) values have been fully utilized. The network average IRI value (\overline{IRI}_{net}) decreased from 4.56 to 1.39 m/km when using a \$2-million budget as indicated by Table 5, which is equivalent to a 69.5% decrease.

Similarly, Table 6 provides sample optimal solutions for maximizing the network average PSI value (\overline{PSI}_{net}) as per Eq. (7) using mean PSI values and the same allocated budget values. It is clear that the same logic outlined earlier has been used in selecting the optimal variables. The optimal variable ($N_{3'}$) with the highest (CE_i) according to Fig. 6 was first selected when allocating a \$0.25-million budget, followed by the variable ($N_{4'}$) with the next highest (CE_i) value when the budget increased to \$0.5-million, and so the same logic continues. The network average PSI value (\overline{PSI}_{net}) increased from 2.49 to 4.01 when using a \$2-million budget as indicated by Table 6, which is equivalent to a 61.0% increase. Figure 7 depicts approximately quadratic relationships between the allocated budget (AB) and deployed pavement condition

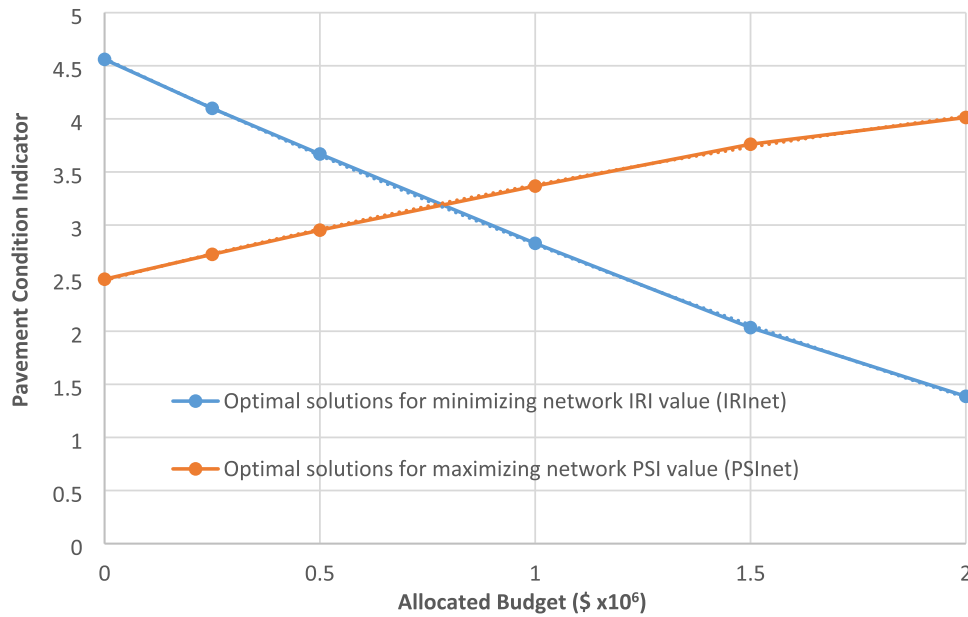


Fig. 7 Sample graphical display of optimal network solutions versus allocated budget

Table 7 Uncertainty impact on optimal \overline{IRI}_{net} and \overline{PSI}_{net} using 99% confidence level

Annual Budget ($\times 10^6$)	Optimal \overline{IRI}_{net} (m/km)					Optimal \overline{PSI}_{net}				
	Upper-limit (UL)	Mean (MN)	Lower-limit (LL)	UE	%E	Upper-limit (UL)	Mean (MN)	Lower-limit (LL)	UE	%E
0.0	4.560	4.560	4.560	0.000	0.00	2.490	2.490	2.490	0.000	0.000
0.25	4.096	4.099	4.103	0.004	0.098	2.725	2.724	2.723	0.001	0.037
0.5	3.662	3.669	3.676	0.007	0.191	2.954	2.952	2.950	0.002	0.068
1.0	2.796	2.828	2.859	0.032	1.132	3.373	3.367	3.362	0.006	0.178
1.5	1.976	2.034	2.088	0.058	2.852	3.773	3.761	3.753	0.012	0.319
2.0	1.322	1.387	1.447	0.065	4.686	4.028	4.013	4.004	0.015	0.374

indicators (i.e., \overline{IRI}_{net} and \overline{PSI}_{net}). Therefore, 2nd-degree polynomial models are obtained using the best-fit technique with very high R-square values as provided in Eqs. (18) and (19). These models can be used to estimate the expected network performance in terms of \overline{IRI}_{net} and \overline{PSI}_{net} as a function of allocated budget (AB).

$$\overline{IRI}_{net} = 0.153AB^2 - 1.901AB + 4.567 (R^2 = 0.9999) \tag{18}$$

$$\overline{PSI}_{net} = -0.126AB^2 + 1.025AB + 2.480 (R^2 = 0.9993) \tag{19}$$

5.3 Uncertainty Analysis

In an effort to investigate the uncertainty impact of IRI measurements on optimal solutions, the optimum rehabilitation model outlined in Eq. (6) has been solved using the upper and lower-limit IRI values (\overline{IRI}_{u_i} & \overline{IRI}_{l_i}) provided in

Table 3 for a 99% confidence level. The corresponding optimal \overline{IRI}_{net} values are provided in Table 7 for the same allocated budgets. Similarly, Eq. (7) has been solved using upper and lower-limit IRI values (\overline{PSI}_{u_i} & \overline{PSI}_{l_i}) provided in Table 3. It can be noticed that the upper-limit solutions in terms of \overline{IRI}_{net} are lower in value while the lower-limit solutions are higher. This is because the \overline{IRI}_{net} is computed by deducting the improvement gains as defined in Eq. (6), thus the upper-limit \overline{IRI}_{u_i} values result in lower-limit \overline{IRI}_{net} values. However, in the case of maximizing the \overline{PSI}_{net} , the upper-limit solutions are higher in value compared to the corresponding lower-limit solutions. Again, the reason is that the improvement gains are added as per Eq. (7) so that the upper-limit \overline{PSI}_{u_i} values result in upper-limit \overline{PSI}_{net} values.

Additionally, Table 7 provides the uncertainty error (UE) defined in Eq. (20) as the maximum difference about the mean value (MN). Table 7 also provides the percent

error (%E) computed as the percentage of uncertainty error (UE) with respect to mean value (MN) as indicated by Eq. (20). It can be noticed from Table 7 that the percent error (%E) is directly proportional to the allocated budget. It has larger values when \overline{IRI}_{net} is minimized compared to when \overline{PSI}_{net} is maximized. The main reason for that is the optimal \overline{IRI}_{net} value gets smaller with the increase in allocated budget while the optimal \overline{PSI}_{net} becomes larger.

$$\%E = \frac{UE}{MN} \times 100\%, \tag{20}$$

where: UE = max. (MN-UL, LL-MN) for IRI

UE = max. (UL-MN, MN-LL) for PSI

MN = mean value, UL = upper-limit value, LL = lower-limit value

Generally, the sample uncertainty errors are relatively small and expected to have a mild impact on the derived optimal solutions. However, the uncertainty errors can be applied to the optimal solutions estimated from Eqs. (18) and (19) so that the uncertainty impact associated with IRI measurements can be reflected.

The presented sample results are obtained using ten independent IRI tests. A question can be raised regarding how many IRI tests are needed to obtain reliable IRI measurements. This question can be answered by assuming one IRI test would be adequate. The answer can be obtained by conducting a statistical hypothesis test seeking to verify that the mean IRI value, \overline{IRI}_i , associated with ten IRI tests is indifferent from the mean IRI value, $\overline{IRI}_{i,j}$, corresponding to the jth IRI test. Equations (21a) and (21b) provide the null and alternative hypotheses, respectively, for the question under consideration.

$$H_0 : \overline{IRI}_i = \overline{IRI}_{i,j} \tag{21a}$$

$$H_a : \overline{IRI}_i \neq \overline{IRI}_{i,j} \tag{21b}$$

The decision can be made by using the t-statistic for two populations with unknown standard deviations. The mean and standard deviation associated with ten IRI tests ($n_1 = 10$) are (\overline{IRI}_i, S_i) as provided in Table 3, while the corresponding statistics associated with one IRI test ($n_2 = 1$) are labeled $(\overline{IRI}_{i,j}, S_{i,j})$. The relevant t-statistic is as defined in Eq. (22) under the assumption of unequal population variances.

$$t = \frac{\overline{IRI}_i - \overline{IRI}_{i,j}}{\sqrt{\frac{S_i^2}{n_1} + \frac{S_{i,j}^2}{n_2}}} \tag{22}$$

The null hypothesis is rejected when the t-value calculated from Eq. (22) is greater than the critical t-value for a two-sided test using 1% significance level and nine degrees of freedom ($t_{\alpha/2} = \pm 3.25$). Table 8 provides sample $(\overline{IRI}_{i,j}, S_{i,j})$ values for pavement classes 1, 3, and 6 considering the IRI data provided in Table 1. Table 8 also provides the corresponding t-statistics computed using Eq. (22). All computed t-statistics are substantially less than the critical t-value of (± 3.25). This means the null hypothesis cannot be rejected in all sample cases presented in Table 8, an indication that the means associated with one and ten IRI tests are statistically indifferent. This is mainly attributed to the large number of measurement points used in the study, which resulted in very similar class means and standard deviations. Therefore, one test is adequate for taking IRI measurements using the IRI-METER-2 device.

Table 8 Computed t-statistics for selected sample means and standard deviations

Test No. (j)	Class 1			Class 3			Class 6		
	\overline{IRI}_i	S_i	t-Stat	\overline{IRI}_i	S_i	t-Stat	\overline{IRI}_i	S_i	t-Stat
	$\overline{IRI}_i=1.63, S_i = 0.27$			$\overline{IRI}_i=4.88, S_i = 0.57$			$\overline{IRI}_i=15.49, S_i = 7.32$		
1	1.600	0.283	0.101	4.901	0.584	- 0.034	15.589	7.632	- 0.012
2	1.593	0.282	0.131	4.908	0.567	- 0.049	14.542	6.312	0.141
3	1.619	0.269	0.039	4.904	0.578	- 0.040	15.888	8.754	- 0.044
4	1.607	0.271	0.081	4.828	0.569	0.087	19.373	9.627	- 0.392
5	1.620	0.279	0.034	4.880	0.568	0.000	15.167	6.948	0.044
6	1.618	0.264	0.043	4.878	0.575	0.003	15.743	7.915	- 0.031
7	1.613	0.274	0.059	4.898	0.577	- 0.030	15.838	8.182	- 0.041
8	1.609	0.280	0.072	4.925	0.571	- 0.075	14.861	6.285	0.094
9	1.623	0.250	0.026	4.802	0.548	0.135	19.770	10.49	- 0.398
10	1.639	0.273	- 0.031	4.914	0.574	- 0.056	14.672	6.552	0.118

6 Conclusions and Recommendations

The presented sample results have indicated the efficacy of the proposed optimum rehabilitation models in yielding optimal solutions at the network-level. In particular, the model designed to use IRI measurements has yielded optimal solutions that resulted in minimizing the network average IRI value, while the model intended to use PSI data has produced optimal solutions that maximized the network average PSI value. Both models seem to provide compatible solutions in terms of optimizing the pavement network conditions. Also, the sample results have indicated the reliability of the proposed cost-effectiveness ratio in identifying the optimal solutions in terms of the numbers of 5-m pavement sections to be rehabilitated using mainly major rehabilitation strategies. This provides the users with a simple and efficient alternative for solving a linear optimum model. The computer software associated with the IRIMETER-2 device provides the user with a colored map displaying the road segments associated with various deployed pavement classes defined using IRI ranges. Therefore, the user seeking to implement a particular optimal solution can easily identify the locations of road segments within each class to be selected for major rehabilitation.

The sample results have also indicated that the uncertainty impact associated with the IRI measurements is very slight when considering the derived optimal solutions, although the impact is found to be linearly proportional to the allocated budget. This implies that more rehabilitation work at the network-level would result in higher risk as one would expect. Additionally, statistical hypothesis testing has revealed that one test would provide IRI means that are indifferent from the means obtained using ten tests for the 6 pavement classes used in the study. Therefore, the recommendation is that one test is adequate. The presented optimum rehabilitation models have been mainly used to generate optimal solutions for a single time-horizon such as a year or two years. While this is typically appropriate for developing countries with limited technical expertise and financial resources, it is recommended to periodically update the derived optimal solutions based on new IRI measurements. This would be facilitated by knowing that a single IRI test is sufficient provided a minimum of 6 pavement classes is used.

The sample highway length of 27.4 km resulted in about 10,840 IRI measurement points, thus providing a good representation of the highway's existing pavement conditions. The statistical analysis performed on the IRI data obtained from ten independent tests resulted in similar class means and standard deviations for both highway directions. This can be considered a good indication that

the amount of available data is adequate to draw valid conclusions. Therefore, it is expected that similar reliable results can be obtained regardless of the network size.

Highway engineers and managers can benefit from this research by first using IRI measurements as part of data inventory, which many highway agencies have already done. They can also adopt the proposed optimum rehabilitation models to be part of their pavement management systems as they are simple to develop and solve at both project and network levels. This would especially be useful for highway engineers seeking to implement pavement management models that are not too complex in terms of data requirements and the generation of optimal solutions. The proposed optimum rehabilitation models are applicable to a single time-horizon such as one year; however, semiannual or annual updates can be easily obtained if a portable profilometer similar to the IRIMETER-2 is used.

The main limitation of the presented optimum rehabilitation models is that they are only valid for a single time-horizon, typically taken as one year or two years. The application of multiple time-horizons requires the incorporation of an appropriate performance prediction model that can be used to predict future IRI records. This can be accomplished once adequate historical IRI records become available. Another limitation is that the proposed models are only applicable to major rehabilitation strategies and inappropriate for the inclusion of routine maintenance treatments typically not expected to cause a major improvement in pavement condition. Finally, the expected initial (IRI_o) value after rehabilitation has been assumed to be the same for all pavement classes; however, this can be revised based on experience and engineering judgment so that a different (IRI_o) value can be assigned to each pavement class.

Data availability The data that support the findings of this study are available from the author upon reasonable request.

Declarations

Conflict of Interest On behalf of all authors, the corresponding author states that there is no conflict of interest.

References

1. Abaza KA (2023) Stochastic-based pavement rehabilitation model at the network level with prediction uncertainty considerations. *Road Mater Pavement Design* 24(11):2680–2698. <https://doi.org/10.1080/14680629.2022.2164330>
2. Abaza KA (2023) Simplified Markovian-based pavement management model for sustainable long-term rehabilitation planning. *Road Mater Pavement Design* 24(3):850–865. <https://doi.org/10.1080/14680629.2022.2048055>

3. Abaza K, Murad M (2009) Predicting flexible pavement remaining strength and overlay design thickness with stochastic modeling. *Transp Res Rec* 2094(1):62–70. <https://doi.org/10.3141/2094-07>
4. Abed A, Thom N, Neves L (2019) Probabilistic prediction of asphalt pavement performance. *Road Mater Pavement Design* 20(Suppl. 1):S247–S264. <https://doi.org/10.1080/14680629.2019.1593229>
5. Santos J, Ferreira A, Flintsch G (2019) An adaptive hybrid genetic algorithm for Pavement management. *Int J Pavement Eng* 20(3):266–286. <https://doi.org/10.1080/10298436.2017.1293260>
6. Abaza KA (2021) Empirical-Markovian approach for estimating the flexible pavement structural capacity: Caltrans method as a case study. *Int J Transp Sci Technol* 10(2):156–166
7. Alaswadko N, Hwayyis K (2022) An approach to investigate the supplementary inconsistency between time series data for predicting road pavement performance models. *Int J Pavement Eng*. <https://doi.org/10.1080/10298436.2022.2045017>
8. Xiao F, Chen X, Cheng J, Yang S, Ma Y (2022) Establishment of probabilistic prediction models for pavement deterioration based on Bayesian neural network. *Int J Pavement Eng*. <https://doi.org/10.1080/10298436.2022.2076854>
9. Park K, Thomas NE, Wayne Lee KJJOTE (2007) Applicability of the international roughness index as a predictor of asphalt pavement condition. *J Transp Eng* 133(12):706–709
10. Fuentes L, Camargo R, Arellana J, Velosa C, Martinez G (2021) Modelling pavement serviceability of urban roads using deterministic and probabilistic approaches. *Int J Pavement Eng* 22(1):77–86
11. Vyas V, Singh AP, Srivastava A (2021) Prediction of asphalt pavement condition using FWD deflection basin parameters and artificial neural networks. *Road Mater Pavement Design* 22(12):2748–2766. <https://doi.org/10.1080/14680629.2020.1797855>
12. Sholevar N, Golroo A, Esfahani SR (2022) Machine learning techniques for Pavement condition evaluation. *Autom Constr* 136:104190. <https://doi.org/10.1016/j.autcon.2022.104190>
13. Saha P, Ksaibati K (2016) A risk-based optimisation methodology for pavement management system of county roads. *Int J Pavement Eng* 17(10):913–923
14. Dalla Rosa F, Liu L, Gharaibeh NG (2017) IRI prediction model for use in network-level pavement management systems. *J Transp Eng, Part B: Pavements* 143(1):04017001
15. Miah MT, Oh E, Chai G, Bell P (2020) An overview of the airport pavement management systems (APMS). *Int J Pavement Res Technol* 13:581–590
16. Issa A, Sammaneh H, Abaza K (2022) Modeling pavement condition index using cascade architecture: classical and neural network methods. *Iran J Sci Technol, Trans Civ Eng* 46(1):483–495
17. Mandiartha P, Duffield CF, Thompson RG, Wigan MR (2012) A stochastic-based performance prediction model for road network pavement maintenance. *Road Transp Res: J Aust N Z Res Pract* 21(3):34–52
18. Yamany MS, Abraham DM (2021) Hybrid approach to incorporate preventive maintenance effectiveness into probabilistic pavement performance models. *J Transp Eng Part B Pavements* 147(1):04020077. <https://doi.org/10.1061/JPEODX.0000227>
19. Abaza KA, Murad MM (2007) Dynamic probabilistic approach for a long-term pavement restoration program with added user cost. *Transp Res Rec* 1990(1):48–56. <https://doi.org/10.3141/1990-06>
20. Mathew BS, Isaac KP (2014) Optimization of maintenance strategy for rural road network using genetic algorithm. *Int J Pavement Eng* 15(4):352–360. <https://doi.org/10.1080/10298436.2013.806807>
21. Khavandi Khiavi A, Mohammadi H (2018) Multi-objective optimization in pavement management system using NSGA-II method. *J Transp Eng, Part B: Pavements* 144(2):04018016. <https://doi.org/10.1061/JPEODX.0000041>
22. Barua L, Zou B (2022) Planning maintenance and rehabilitation activities for airport pavements: a combined supervised machine learning and reinforcement learning approach. *Int J Transp Sci Technol* 11(2):423–435
23. Sayers MW, Gillispie TD, Queiroz C (1986) The international road roughness experiment: establishing correlation and a calibration standard for measurements. The World Bank, Washington, DC
24. Múčka P (2019) Influence of profile specification on international roughness index. *J Infrastruct Syst* 25(2):04019005
25. Huang Y (2004) Pavement analysis and design, 2nd edn. Pearson/Prentice Hall, Upper Saddle River, NJ
26. Zeng J, Gül M, Mei Q (2022) A computer vision-based method to identify the international roughness index of highway pavements. *J Infrastruct Intell Resil* 1(1):100004
27. Múčka P (2017) International roughness index specifications around the world. *Road Mater Pavement Design* 18(4):929–965
28. Sidess A, Ravina A, Oged E (2022) A model for predicting the deterioration of the international roughness index. *Int J Pavement Eng* 23(5):1393–1403
29. Šroubek F, Šorel M, Žák J (2022) Precise international roughness index calculation. *Int J Pavement Res Technol* 15:1413–1419
30. Mirtabar Z, Golroo A, Mahmoudzadeh A, Barazandeh F (2022) Development of a crowdsourcing-based system for computing the international roughness index. *Int J Pavement Eng* 23(2):489–498
31. Abdelaziz N, Abd El-Hakim RT, El-Badawy SM, Afify HA (2020) International roughness index prediction model for flexible pavements. *Int J Pavement Eng* 21(1):88–99
32. Pérez-Acebo H, Bejan S, Gonzalo-Orden H (2018) Transition probability matrices for flexible pavement deterioration models with half-year cycle time. *Int J Civ Eng* 16(9):1045–1056
33. Khattak MJ, Nur MA, Bhuyan MRUK, Gaspard K (2014) International roughness index models for HMA overlay treatment of flexible and composite pavements. *Int J Pavement Eng* 15(4):334–344
34. Loprencipe G, Pantuso A, Di Mascio P (2017) Sustainable pavement management system in urban areas considering the vehicle operating costs. *Sustainability* 9(3):453
35. Saha P, Ksaibati K (2016) A risk-based optimisation methodology for pavement management system of county roads. *Int J Pavement Eng, Eng* 17(10):913–923
36. Janani L, Dixit RK, Sunitha V, Mathew S (2020) Prioritisation of pavement maintenance sections deploying functional characteristics of pavements. *Int J Pavement Eng* 21(14):1815–1822
37. Khattak MJ, Baladi GY, Zhang Z, Ismail S (2008) A review of the pavement management system of the state of Louisiana-Phase I. *Transp Res Rec: J Transp Res Board* 2084:18–27
38. Nassiri S, Shafiee MH, Bayat A (2013) Development of roughness prediction models using Alberta transportation's pavement management system. *Int J Pavement Res Technol* 6(6):714
39. Paterson W (1986) International roughness index: relationship to other measures of roughness and riding quality. *Transp Res Rec: J Transp Res Board* 1084:49–58
40. Al-Omari B, Darter MI (1994) Relationships between international roughness index and present serviceability rating. *Transp Res Record: J Transp Res Board* 1435:130–136
41. ASTM (2007) Standard practice for roads and parking lots, pavement condition index surveys. ASTM D6433–07. West Conshohocken, PA: ASTM
42. Dewan SA, Smith RE (2002) Estimating IRI from pavement distresses to calculate vehicle operating costs for the cities and

- counties of San Francisco Bay area. *Transp Res Rec: J Transp Research Board* 1816:65–72
43. American Association of State Highway and Transportation Officials (AASHTO) (1993) AASHTO guide for design of pavement structures. AASHTO, Washington, DC
44. Elhadidy AA, El-Badawy SM, Elbeltagi EE (2021) A simplified pavement condition index regression model for pavement evaluation. *Int J Pavement Eng* 22(5):643–652
45. Adeli S, Najafi M, Gilani V, Kashani Novin M, Motesharei E, Salehfard R (2021) Development of a relationship between pavement condition index and international roughness index in rural road network. *Adv Civ Eng*. <https://doi.org/10.1155/2021/6635820>
46. Plati C, Gkyrtis K, Loizos A (2023) A practice-based approach to diagnose pavement roughness problems. *Int J Civ Eng*. <https://doi.org/10.1007/s40999-023-00900-x>
47. Abaza KA, Assi NA (2023) The use of IRI data in developing optimal pavement rehabilitation plan for developing countries: Palestine as a case study. Preprint, Research- square

Springer Nature or its licensor (e.g. a society or other partner) holds exclusive rights to this article under a publishing agreement with the author(s) or other rightsholder(s); author self-archiving of the accepted manuscript version of this article is solely governed by the terms of such publishing agreement and applicable law.